Published in final edited form as:
Biomaterials. 2011 November ; 32(31): 7905–7912. doi:10.1016/j.biomaterials.2011.07.001.

3D *in vitro* bioengineered tumors based on collagen I hydrogels

Christopher S. Szot[*], **Cara F. Buchanan**, **Joseph W. Freeman**, and **Marissa N. Rylander**
School of Biomedical Engineering and Sciences, Virginia Tech-Wake Forest University, Blacksburg, VA 24061, USA

Abstract

Cells cultured within a three-dimensional (3D) *in vitro* environment have the ability to acquire phenotypes and respond to stimuli analogous to *in vivo* biological systems. This approach has been utilized in tissue engineering and can also be applied to the development of a physiologically relevant *in vitro* tumor model. In this study, collagen I hydrogels cultured with MDA-MB-231 human breast cancer cells were bioengineered as a platform for *in vitro* solid tumor development. The cell–cell and cell-matrix interactions present during *in vivo* tissue progression were encouraged within the 3D hydrogel architecture, and the biocompatibility of collagen I supported unconfined cellular proliferation. The development of necrosis beyond a depth of ~150–200 μm and the expression of hypoxia-inducible factor (HIF)-1α were demonstrated in the *in vitro* bioengineered tumors. Oxygen and nutrient diffusion limitations through the collagen I matrix as well as competition for available nutrients resulted in growing levels of intra-cellular hypoxia, quantified by a statistically significant ($p < 0.01$) upregulation of HIF-1α gene expression. The bioengineered tumors also demonstrated promising angiogenic potential with a statistically significant ($p < 0.001$) upregulation of vascular endothelial growth factor (VEGF)-A gene expression. In addition, comparable gene expression analysis demonstrated a statistically significant increase of HIF-1α ($p < 0.05$) and VEGF-A ($p < 0.001$) by MDA-MB-231 cells cultured in the 3D collagen I hydrogels compared to cells cultured in a monolayer on two-dimensional tissue culture polystyrene. The results presented in this study demonstrate the capacity of collagen I hydrogels to facilitate the development of 3D *in vitro* bioengineered tumors that are representative of the pre-vascularized stages of *in vivo* solid tumor progression.

Keywords

Collagen I; Hydrogel; Three-dimensional; Tumor microenvironment; Hypoxia

1. Introduction

Cancer biologists, biomedical researchers, and oncologists have long relied on two-dimensional (2D) Petri dish studies and small animal models to study the complex tumorigenic mechanisms of angiogenesis, invasion, and metastasis. However, these models of tumor development have thus far been inadequate for cultivating the discovery of definitive cancer termination and prevention treatments. 2D cell culture models lack the structural architecture necessary for proper cell–cell and cell-matrix interactions and are therefore incapable of replicating an *in vivo* phenotype [1–5]. Small animal models are the current gold standard for conducting cancer research, even though there are considerable differences between cancer progression in humans and animals [3,6]. Additionally, animals intrinsically contain many uncontrollable factors, including host cells, an immune response,

[*]Corresponding author. Tel.: +1 540 231 0636; fax: +1 540 231 9738. szotc@vt.edu (C.S. Szot).

hemodynamics, and endogenous growth factors. These variables complicate isolating the impact of specific stimuli, such as cellular, chemical, and mechanical cues, during therapeutic testing [7]. Recently, some promising three-dimensional (3D) cell culture models have been developed for studying tumor progression *in vitro*. Results in the literature show that these models are beginning to restore the cellular morphologies and phenotypes seen during *in vivo* tumor development [8–13].

Ghajar and Bissell recently defined Tumor Engineering as "the construction of complex culture models that recapitulate aspects of the *in vivo* tumor microenvironment to study the dynamics of tumor development, progression, and therapy on multiple scales [14]." This burgeoning field of research is rapidly evolving the study of cancer progression *in vitro* [5,15]. Fischbach and colleagues have engineered an array of 3D *in vitro* tumor models using both synthetic and natural polymeric scaffolds to demonstrate angiogenic factor secretion and drug responsiveness [8], the effects of tumor oxygen tension and 3D cell-extracellular matrix (ECM) interactions on angiogenic potential [12], and endothelial cell remodeling of dense collagen I matrices in response to potential secretion of angiogenic factors from underlying cancer cells [9]. Nelson and Bissell have highlighted the importance of developing functional 3D *in vitro* models of mammary gland acini for advancing breast cancer research [10] and have fabricated 3D epithelial culture models using lithography [11]. Our group has reported previously on the potential use of nanofibrous scaffolds, such as bacterial cellulose and electrospun polymer composites, for tissue engineering *in vitro* tumor models [16].

The pre-vascularized stages of solid tumor growth can be characterized by identifiable criteria within the tumor microenvironment, including an uninhibited 3D proliferative capacity [17], regions of hypoxia surrounding a necrotic core [18,19], and activation of genetic factors that lead to the recruitment of local endothelial cells for self-sustaining angiogenesis (Fig. 1a) [17,20]. Uninhibited 3D proliferative capacity is a trait that cancer cells achieve during *in vivo* tumor development following a series of mutations that cause growth signal autonomy, insensitivity to antigrowth signals, and resistance to apoptosis [17]. Cancer cell lines *in vitro* maintain this phenotype, demonstrating limitless proliferation within the confines of their environment. Culturing cancer cells in 3D scaffolds has been shown to foster this proliferative potential, allowing for growth of clinically relevant tumor masses [8]. However, within an *in vivo* tumor microenvironment, there are restrictions on tumor growth enforced by oxygen and nutrient diffusion limitations through tissue. Hypoxia, a state of limited oxygen availability, occurs within 100–200 μm of the closest vasculature. Cancer cells that cannot adjust to the oxygen and nutrient deficiencies at the core of a growing tumor mass cede to cell death through either apoptosis or necrosis. A key marker for identifying hypoxia is hypoxia-inducible factor (HIF)-1α, a heterodimeric transcription factor protected from degradation when the surrounding oxygen tension is at a hypoxic level [18,19]. Solid tumors evolve from an avascular to a vascular state by responding to this microenvironmental hypoxic stress and initiating an angiogenic response from the host vasculature. This process is instigated by the cancer cells, which secrete growth factors and cytokines that interact with local endothelial cells, promoting vascular sprouting and neovascularization [21]. Vascular endothelial growth factor A (VEGF-A), a heparin-binding homodimeric glycoprotein, plays a major role in initiating this process through stimulating vascular permeability and endothelial growth [22]. Activation of VEGF-A gene transcription occurs in direct response to the development of hypoxia and HIF-1α expression [23].

The biocompatibility and 3D architecture of collagen I hydrogels are suitable properties for reproducing the microenvironmental conditions of a solid tumor. Collagen I is a frequently used substrate for cell culture and tissue engineering applications, because it contains the tripeptide RGD (Arg-Gly-Asp), a short amino acid sequence that preferentially binds to

receptors on cell surfaces [24]. Cell-mediated degradation of collagen I through the secretion of cleaving enzymes allows for remodeling of the matrix during proliferation, migration, and infiltration [25]. Furthermore, hydrogel concentration, scaffold thickness, and cell seeding density can be tailored to stimulate specific cellular responses within the engineered microenvironment. We hypothesize that collagen I hydrogels can be used as 3D cell culture scaffolds for bioengineering tumors that mimic key characteristics of *in vivo* tumor progression.

While the infiuence of hypoxic oxygen levels and cell-matrix interactions on the angiogenic potential of cancer cells cultured *in vitro* has been documented [12], a 3D *in vitro* tumor microenvironment that inherently promotes a phenotype typical of the pre-vascularized stages of *in vivo* solid tumor progression has not been established. In this study, MDA-MB-231 human breast cancer cells were cultured in collagen I hydrogel scaffolds, and the cell–cell and cell-matrix interactions present during *in vivo* development were demonstrated. Culturing conditions, including cell seeding density and scaffold thickness, were varied to control oxygen and nutrient availability and diffusion limitations for the purpose of encouraging the development of necrosis and hypoxia. These phenotypical changes were confirmed through real-time fluorescent imaging, immunofluorescence staining, and gene expression analysis. The bioengineered tumors exhibited considerable angiogenic potential, with a statistically significant upregulation of VEGF-A gene expression in response to the growing levels of intra-cellular hypoxia. The results from this study support the development of 3D *in vitro* bioengineered tumors that are representative of *in vivo* tumor progression.

2. Materials and methods

2.1. Cell culture

The MDA-MB-231 human breast cancer cell line was used in all experiments (American Type Culture Collection, Manassas, VA, USA). MDA-MB-231 cells were cultured in GIBCO® DMEM/F12 (1:1) +L-Glutamine, +15 mM HEPES (Invitrogen, Carlsbad, CA, USA) and supplemented with 10% fetal bovine serum (Sigma Aldrich, St. Louis, MO, USA) and 1% Penicillin/Streptomycin (Invitrogen). Cell cultures were incubated in a humidified atmosphere of 95% air and 5% CO_2 at a constant temperature of 37 °C. Cell passages of 10–18 were used for all experiments.

2.2. Collagen I Hydrogels

Collagen I was removed from rat tail tendons and prepared as a solid hydrogel to facilitate 3D cell culture. Tendons were excised from the tails of Sprague Dawley rats and allowed to dissolve in 40 ml of 10 mM HCl per gram of tendon under agitation overnight at room temperature. The resulting suspension was centrifuged at 30,000 g for 30 min at 4 °C. The supernatant, containing the collagen I, was decanted and the pellet was discarded. The concentration of collagen I was obtained by evaporating out the solvent from 0.25, 0.5, and 1.0 ml samples in a 110 °C oven for 2 h, measuring the dry weights, and averaging the concentration values. In order to sterilize the collagen I for cell culture, chloroform (10% of the volume of collagen) was layered beneath the collagen I solution and allowed to rest for 24 h at 4 °C (Sigma Aldrich protocol).

The volume of collagen I necessary for obtaining a target final concentration of 8 mg/ml was neutralized with a buffer containing 10× concentrated DMEM (supplemented with 4.5 g/L glucose, L-glutamine, sodium pyruvate, and sodium bicarbonate; Mediatech, Inc., Manassas, VA, USA), 1N NaOH, and dH_20. In order to initiate collagen I gelation, the ratio of components in the neutralizing buffer was calculated using the following equations: (1) 10×

DMEM = Final Volume × 0.1, (2) 1N NaOH = Volume of Collagen I × 0.02, and (3) dH_20 = Final Volume − Volume of Collagen I – 10× DMEM – 1N NaOH. MDA-MB-231 cells were first suspended in the neutralizing buffer and then mixed with the collagen I solution at the desired final seeding density (Fig. 1b). The collagen-cell suspension was pipetted into 8 mm diameter cylindrical glass molds and allowed to gel in an incubator at 37 °C for 30 min. The volume of the collagen-cell suspension (75 and 150 μl) was varied to fabricate specific levels of hydrogel thickness (1.5 and 3 mm, respectively). The cancer cell seeded hydrogels were removed from the molds and cultured in cell culture media, as described above, for 0, 1, 3, 5, and 7 days.

2.3. Immunofluorescence staining

The bioengineered tumors were fixed in 10% formalin for 24 h at room temperature and then stored in 70% ethanol (EtOH) for no longer than 7 days at 4 °C. Next, the tumors were dehydrated through a series of EtOH incubations (70, 80, 90, 95, 95, 100, 100%) at 37 °C and then moved to xylene for 1 h at room temperature. A series of two 1 h melted paraffin wax (Tissue Prep, Fischer Scientific, Pittsburgh, PA, USA) incubations at 60 °C were used to embed the bioengineered tumors, and the wax blocks were allowed to solidify overnight at 4 °C. A Microm HM 355S microtome (Thermo Scientific, Kalamazoo, MI, USA) was used to obtain 15 μm thick sections. Paraffin was removed from the slides using a pair of xylene washes followed by a series of EtOH washes (100, 100, 95, 95, 80%) to re-hydrate the tumor sections. All images shown are representative of the entire bioengineered tumor.

2.3.1. 3D Morphological Analysis—Cell morphology was analyzed as described previously [16]. Briefly, bioengineered tumor sections were permeabilized using 0.5% Triton X-100 (Sigma Aldrich), and 1% BSA (Santa Cruz Biotechnology Inc., Santa Cruz, CA, USA) was used as a blocking buffer for 30 min at 37 °C. Cells were stained for 20 min at room temperature with rhodamine phalloidin (Invitrogen), a high-affinity probe for F-actin, and sections were mounted with VECTASHIELD® mounting medium with DAPI (Vector Laboratories, Burlingame, CA, USA), to visualize nuclei. Imaging was performed using a Zeiss LSM 510 laser scanning confocal microscope (Carl Zeiss, Thornwood, NY, USA).

2.3.2. Cell proliferation and necrosis—Cell proliferation was qualitatively observed using a DAPI stain for nuclei, as described above. A Leica DMI 6000 fluorescent microscope (Leica Microsystems Inc., Buffalo Grove, IL, USA) was used to tile a set of images and reconstruct entire cross sections of the bioengineered tumors. Representative ~2 mm^2 regions of interest are shown. The development of necrosis and the depth at which this occurred was analyzed using a laser scanning confocal microscope (Zeiss LSM 510) to perform a Z-stack through a “live” bioengineered tumor in real-time. Image slices were taken at intervals of 5–10 μm to a depth of ~400 μm. Prior to imaging, the bioengineered tumors were incubated for 45 min in cell culture media containing 4 μM calcein AM (λ_{em} = 515 nm, Invitrogen) to stain viable cells. 1.5 mM propidium iodide (λ_{em} = 617 nm, Invitrogen) was added to the cell culture media for the last 5 min of the calcein AM incubation to stain dead cells. The bioengineered tumors were washed with PBS before imaging.

2.3.3. Hypoxia—The presence of hypoxia was visualized using a rabbit monoclonal [EP1215Y] to HIF-1α primary antibody (Abcam Inc., Cambridge, MA, USA) in conjunction with an Alexa Fluor® 350 goat anti-rabbit IgG (H + L) secondary antibody (Invitrogen). Bioengineered tumor sections were permeabilized with 0.5% Triton X-100 (Sigma Aldrich) and blocked with 5% goat serum (Santa Cruz Biotechnology Inc.) overnight at 4 °C. Sections were incubated at 37 °C for 2.5 h with the HIF-1α primary antibody and then for 1

h with the Alexa Fluor® 350 secondary antibody, separated by a series of PBS washes. VECTASHIELD® mounting medium was used to preserve fluorescence. Sections were imaged with a Leica DMI 6000 fluorescent microscope. The fluorescent images were overlaid on the bright field images.

2.4. Gene expression analysis

The gene expression levels of HIF-1α and VEGF-A were measured using quantitative reverse transcription polymerase chain reaction (qRT-PCR). Total RNA was first isolated on days 0, 1, 3, 5, and 7 using TRI Reagent® Solution (Applied Biosystems/Ambion, Austin, TX, USA). For the 3D cell culture groups, the cells were allowed to remain in culture for 4 h on day 0 before RNA isolation was performed. For the 2D cell culture group, the cells were allowed to remain in culture for 8 h to ensure complete cell attachment before RNA isolation was performed. Next, 1 μg of total RNA was reverse-transcribed to cDNA using a Reverse Transcription System (Promega, Madison, WI, USA). Lastly, an ABI 7300 Sequence Detection System (Applied Biosystems, Carlsbad, CA, USA) was used to conduct qRT-PCR using TaqMan® Universal PCR Master Mix and gene-specific TaqMan® PCR primers (Applied Biosystems): HIF-1α (NM_001530.3), VEGF-A (NM_001025366.2), and GAPDH (NM_002046.3). Gene expression was normalized to GAPDH using the comparative threshold cycle (ΔΔCt) method of quantification [26]. The data is presented as a relative fold induction, calculated as $2^{-\Delta\Delta C_T}$, with gene expression on day 0 used as the control group in Fig. 5 and gene expression for 2D cell culture used as the control group in Fig. 6. All experiments were performed with an $n = 4$.

2.5. Statistical Analysis

Gene expression levels measured by qRT-PCR were analyzed for significance using an ANOVA test with a Tukey post hoc test. $p < 0.05$ was considered significant, and $p < 0.01$ and $p < 0.001$ were also noted.

3. Results

3.1. Cell morphology in 3D collagen I hydrogels

MDA-MB-231 cells were cultured in 3D collagen I hydrogels for 1, 3, 5, and 7 days (Fig. 2a–d, respectively). The cells developed a stellate, elongated morphology with disorganized nuclei and invasive processes by day 3, demonstrating cell-matrix interactions (Fig. 2b). By day 5, as the cells began to proliferate throughout the hydrogel, they aggregated into clusters, demonstrating cell–cell interactions (Fig. 2c). These cell-matrix and cell–cell interactions are representative of *in vivo* biological systems and have been classified previously [27].

3.2. Cell proliferation and the progression towards cell death

Proliferation of MDA-MB-231 cells, seeded at a density of 1 million cells/ml in 3 mm thick collagen I hydrogels, was qualitatively observed using a DAPI stain. Representative ~2 mm^2 regions of interest are shown from the bioengineered tumor cross sections. On day 1, the cells appear to be evenly distributed throughout the entire volume of the hydrogel (Fig. 3a). A noticeable increase in cell number was visible from day 1 to day 5, with numerous cell clusters forming by day 5 (Fig. 3b). On day 5, the cell clusters were evenly distributed, similar to the individual cells on day 1, suggesting that they formed as a result of cell proliferation rather than cell migration.

In an effort to induce necrosis at the core of the bioengineered tumors, MDA-MB-231 cells were seeded at a higher density of 4 million cells/ml in 3 mm thick collagen I hydrogels. On day 1, viable cells were visible and evenly distributed throughout the entire 400-μm segment

with only a small number of dead cells present at non-specific degrees of depth (Fig. 3c). However, on day 5, viable cells were only visible until a depth of ~150–200 μm from the bioengineered tumor surface (Fig. 3d). Beyond this level, a large number of dead cells were present followed by a large void with no visible cells. Cell death was attributed to limitations in oxygen and nutrient diffusion through the collagen I matrix and an increase in consumption of the available nutrients. One explanation for the cellular void at the core of the bioengineered tumors is that since propidium iodide is a nuclear stain, the nuclear DNA degraded in the dead cells closest to the center [28]. Another possibility is that the cells migrated to the outer periphery of the bioengineered tumors towards the more prevalent supply of oxygen and nutrients.

3.3. Growing levels of hypoxia in the bioengineered tumors

The onset of tumor necrosis is a direct result of limited oxygen and nutrient availability [18,19]. Therefore, hypoxia is a viable precursor of cell death. To demonstrate this correlation, MDA-MB-231 cells were seeded at a density of 4 million cells/ml in 3 mm thick hydrogels, similar to the experiment used to induce necrosis. Intra-cellular levels of hypoxia were qualitatively observed through immunofluorescence imaging of HIF-1α protein. HIF-1α was visible on day 1 (Fig. 4a) with an increase in intensity seen on day 5 (Fig. 4b). The presence of HIF-1α on day 1 demonstrates the initial hypoxic cellular response to being cultured in 3D. It is expected that cells will have greater difficulty in obtaining oxygen and nutrients when confined within a 3D matrix as opposed to being cultured in a monolayer where they are in direct contact with oxygenated media. The increase in HIF-1α intensity observed on day 5 was attributed to cell proliferation and the resulting increase in competition for available oxygen and nutrients. This was evident in the large clusters of cells, which exhibited the greatest magnitude of intensity, signifying an augmented degree of intra-cellular hypoxia [22].

3.4. Bioengineered tumor hypoxic and angiogenic gene expression profile

In order to demonstrate an intrinsically induced upregulation of HIF-1α and VEGF-A gene expression in correlation with bioengineered tumor maturation, we varied scaffold thickness and cell seeding density to alter specific microenvironmental parameters including oxygen and nutrient diffusion and competition for available nutrients. Three culturing configurations were used: 4 million cells/ml seeded in 3 mm thick hydrogels (Fig. 5a and b), 1 million cells/ml seeded in 3 mm thick hydrogels (Fig. 5c and d), and 4 million cells/ml seeded in 1.5 mm thick hydrogels (Fig. 5e and f).

When 4 million cells/ml were seeded in the thicker, 3 mm hydrogels, HIF-1α expression was upregulated on day 3 and day 5 (Fig. 5a). Although this upregulation was not statistically significant compared to day 0, immunofluorescence staining (Fig. 4) demonstrated an initial presence of HIF-1α protein on day 1 with an increase in intensity on day 5. The statistically significant ($p < 0.01$) decrease in HIF-1α gene expression on day 7 is hypothesized to be a result of the hypoxic cells dying from a lack of oxygen and nutrients. VEGF-A expression was statistically upregulated ($p < 0.001$) on days 3, 5, and 7 compared to day 0 (Fig. 5b). Between day 3 and day 5, VEGF-A expression was further significantly upregulated ($p < 0.001$), whereas between day 5 and day 7, VEGF-A expression was significantly downregulated ($p < 0.001$). However, day 7 VEGF-A expression was still significantly higher compared to day 0. Since HIF-1α expression leads to activation of VEGF-A gene transcription [23], this decrease in VEGF-A expression from day 5 to day 7 was likely due to the downregulation in HIF-1α expression seen on day 7.

When the cell seeding density was reduced to 1 million cells/ml in the 3 mm thick hydrogels, the competition for available oxygen and nutrients decreased, resulting in an

initial downregulation of HIF-1α expression (Fig. 5c) and a delayed upregulation of VEGF-A expression (Fig. 5d), compared to when 4 million cells/ml were seeded in the same scaffold thickness. HIF-1α expression was significantly upregulated ($p < 0.05$) on day 3 and day 5 compared to day 1 and significantly upregulated ($p < 0.01$) on day 7 compared to day 0. VEGF-A expression was significantly upregulated on day 3 ($p < 0.05$) and days 5 and 7 ($p < 0.001$) compared to day 0. Between day 3 and day 5 and between day 5 and day 7, VEGF-A expression was further significantly upregulated ($p < 0.01$ and $p < 0.001$, respectively). When comparing data from the high (4 million cells/ml) and low (1 million cells/ml) cell seeding densities in 3 mm thick bioengineered tumors, it can be concluded that HIF-1α and VEGF-A gene expression upregulation peaked at day 5 when a high seeding density was used as a result of oxygen and nutrient deficiency-induced cell death after day 5 (Fig. 5a and b). However, with a lower seeding density, a consistent upregulation is present over the 7-day period, indicative of cell proliferation-sustained hypoxic stresses (Fig. 5c and d).

Decreasing the scaffold thickness to 1.5 mm mitigated the oxygen and nutrient diffusion limitations. Under these culturing conditions, neither HIF-1α nor VEGF-A expression were upregulated on any day compared to day 0 (Fig. 5e and f). HIF-1α expression was significantly downregulated ($p < 0.01$) on day 1 and maintained that level through day 7. As mentioned previously, since HIF-1α expression is known to activate VEGF-A gene transcription [23], no significant upregulation in VEGF-A expression compared to day 0 was expected. An increase in intra-cellular hypoxic levels is expected when cells are first confined in a 3D matrix on day 0. Therefore, the significant downregulation in HIF-1α expression seen on day 1 implies that the cells had migrated to the periphery of the bioengineered tumors to obtain more oxygen.

3.5. 2D versus 3D cell culture: comparison of hypoxic and angiogenic gene expression

Comparable gene expression analysis between cells cultured in a 2D monolayer versus in a 3D hydrogel was performed to emphasize the importance and relevance of using 3D cell culture models. Fig. 6 demonstrates a statistically significant upregulation of HIF-1α ($p < 0.05$) and VEGF-A ($p < 0.001$) gene expression when MDA-MB-231 cells were cultured in the 3D collagen I hydrogels compared to a 2D 6-well cell culture dish. Since HIF-1α and VEGF-A expression were shown to change over time due to microenvironmental conditions (Fig. 5), gene expression was compared on day 0 to determine the specific effect of 3D cell culture on the phenotypic changes. This initial upregulation of HIF-1α gene expression in the 3D bioengineered tumors is consistent with the presence of HIF-1α protein on day 1 (Fig. 4a) and supports the cell migration-mediated downregulation of HIF-1α gene expression observed in the thinner scaffolds on day 1 (Fig. 5e).

4. Discussion

The development and utilization of 3D *in vitro* cell culture models for studying the complex mechanisms of tumorigenesis are beginning to play a major role in advancing fundamental cancer research as well as the testing and discovery of several different treatment modalities. The field of tissue engineering offers a promising approach for fabricating “functional” *in vitro* tumor models that are representative of *in vivo* tumor progression. Similar to tissue engineering an organ or tissue replacement, cells are grown on 3D polymeric scaffolds in an *in vitro* environment that induces upregulation of characteristic genetic markers, HIF-1α and VEGF-A in this study, to promote an *in vivo* phenotype. Our previous work has investigated electrospun polycaprolactone/collagen I composites as a scaffold for *in vitro* tumor development [16]. While the electrospun scaffolds demonstrated favorable cell adhesion, viability, and proliferation, the fibers were too compact to allow for significant cell infiltration and 3D growth. Other attempts by our group have involved the fabrication of 3D electrospun poly(L-lactic) acid/polyethylene oxide (PEO) composite scaffolds where the

PEO was leached out, leaving large pores for cell infiltration [29]. Although significant cell infiltration and 3D growth was achieved over several weeks, the development of intra-cellular levels of hypoxia was not observed.

In the present study, collagen I hydrogel scaffolds facilitated immediate 3D cell growth, allowing for the development of necrotic and hypoxic cellular regions. A collagen I concentration of 8 mg/ml was chosen based on mechanical characterization data from the literature [30]. Paszek et al. measured the elastic moduli of established tumors grown in transgenic mice as well as hydrogels containing 2 and 4 mg/ml collagen I, with values reported of 4.05 ± 0.94 kPa, 0.328 ± 0.09 kPa, and 1.59 ± 0.38 kPa, respectively. We expect an 8 mg/ml collagen I hydrogel to have an elastic modulus that falls within the range of the established tumor models. Matrix stiffness is an important microenvironmental parameter, because it directly affects cell-matrix interactions, including cell infiltration and matrix remodeling during cell proliferation [31,32]. In addition to controlling stiffness, the concentration of collagen I also determines the diffusivity of the hydrogel matrix [30,33], which is an important factor in the development of hypoxia [19,31,32]. Using a collagen I-based hydrogel promoted ideal cell adhesion, viability, and proliferation. Cells demonstrated visible, invasive processes that interacted with the surrounding matrix, and the cell-mediated degradation of collagen I allowed for uninhibited cell proliferation and the formation of large cell clusters (Figs. 2 and 3a and b). As opposed to when cells are cultured in 2D, these cell-matrix and cell–cell interactions encourage cell signaling and a phenotype representative of *in vivo* biological systems [1,2].

Analogous to *in vivo* tumor progression, limitations in oxygen and nutrient diffusion through the collagen I matrix as well as increased competition for the available nutrients, led to cell death beyond a depth of ~150–200 μm from the surface of the bioengineered tumors and an increase in intra-cellular levels of hypoxia (Figs. 3d and 4). The restriction of viable cells to a ~150–200 μm region below the bioengineered tumor surface is representative of the oxygen diffusion limitations in biological tissue [19] and has been shown previously in collagen I hydrogels [34]. HIF-1α protein and gene expression analysis were used to determine hypoxia given that the degree of HIF-1α expression correlates with intra-cellular oxygen levels [22]. Immunofluorescence staining demonstrated expression of HIF-1α protein on day 1 with a noticeable increase in intensity correlating with cell proliferation on day 5, in culturing conditions using a high cell seeding density (4 million cells/ml, 3 mm thick scaffolds) (Fig. 4). HIF-1α gene expression was significantly upregulated at the lower cell seeding density (1 million cells/ml, 3 mm thick scaffolds) over the 7-day culturing period (Fig. 5c), though immunofluorescence intensity was only observed to be slightly greater than the background (data not shown). This indicated that while HIF-1α gene expression was not significantly upregulated over time at the higher cell seeding density, the initial degree of intra-cellular hypoxia was greater than at the lower cell seeding density. Intra-cellular hypoxic levels were also shown to be initially upregulated on day 0 when cells were cultured in 3D as opposed to 2D (Fig. 6a). Our results suggest that this is a consequence of diffusion limitations and competition for the available oxygen and nutrients in the immediate vicinity within the confined 3D collagen I matrix. When a thinner hydrogel scaffold was used (1.5 mm thick), HIF-1α was significantly downregulated on day 1 (Fig. 5e), implying that the cells were no longer experiencing the same hypoxic oxygen tension as on day 0. We believe this is a result of the cells migrating towards the periphery of the scaffold, where more oxygen was available. Overall, cells cultured in 3D were shown to experience initial intra-cellular levels of hypoxia on day 0, with a larger cell seeding density correlating with a greater degree of hypoxia and an increase in HIF-1α expression associated with cell proliferation and the aggregation of cells into large clusters.

The developed intrinsic increase in intra-cellular hypoxic oxygen levels led to a statistically significant upregulation of VEGF-A gene expression (Fig. 5B, D), which is a strong indicator of the angiogenic potential of the *in vitro* bioengineered tumors. Achieving a hypoxic microenvironment was important for reproducing the *in vivo* stages of tumor development, specifically the HIF-1α expression-mediated activation of VEGF-A gene transcription [23]. Our results are representative of this, with a direct correlation between HIF-1α and VEGF-A expression demonstrated in all gene expression experiments (Figs. 5 and 6). VEGF-A is a crucial factor involved in tumor maturation, acting exclusively on endothelial cells to promote tumor angiogenesis [21,22]. Hence, the significant upregulation of VEGF-A expression induced in the *in vitro* bioengineered tumors points towards the accuracy and relevance of our model. Similar 3D *in vitro* cancer cell culture systems have also shown an upregulation in VEGF-A expression in response to both hypoxic oxygen levels and 3D cell-matrix interactions [12]. These systems, however, relied upon the use of manufactured airflow to reproduce a hypoxic environment, rather than allowing cell proliferation and matrix-imposed limitations in oxygen and nutrient diffusion to foster the development of hypoxic oxygen levels.

Although this bioengineered tumor model is only a simplistic representation of the complex nature of a malignant tumor, several key characteristics of *in vivo* solid tumor development (e.g. necrosis, hypoxia, angiogenic gene upregulation) were reproduced, thus exposing the cells to typical tumor microenvironmental stresses. Therefore, it is believed that the *in vitro* bioengineered tumors will respond to stimuli comparable to an *in vivo* response, allowing this system to be used as a more efficient tool for testing a wide range of treatment modalities over conventional methods [35]. The advantages of using 3D scaffolds over 2D tissue culture polystyrene for obtaining an *in vivo* phenotype are well documented [1–5]. However, small animal models are still the primary vehicles used for determining drug efficacy. One of the main issues with drug testing in animals is that many new drugs have success in animal pre-clinical trials but fail in human clinical trials, wasting significant time and money [36]. This failure stems from significant cellular and genetic differences between humans and animals [6]. In addition, the ethical and humane issues associated with animal trials are a noteworthy concern. Nevertheless, animal models should still be used during pre-clinical trials but in conjunction with 3D cell culture systems. Substantial progress still needs to be made before 3D *in vitro* tumor models can replace the more physiologically complete and familiar small animal models.

Physiologically relevant 3D cell culture models, such as the one developed in this study, have the potential to aide in accelerating more effective and cost efficient drug discovery. The next step in advancing our *in vitro* bioengineered tumors into more complex, “functional” tumor replicates is to incorporate additional cell types, including endothelial and stromal cells, to induce neovessel formation. Engineering an *in vitro* 3D microenvironment in which the malignant, tumorigenic mechanisms of angiogenesis, invasion, and metastasis can mature through a natural progression will yield a cell culture system with greater and more reliable predictive capability than traditional animal models. The pre-vascularized bioengineered tumor model introduced in this study is the first step towards tissue engineering a “functional” cancer model.

5. Conclusion

The results presented in this study demonstrate that collagen I hydrogels can facilitate the pre-vascularized stages of *in vivo* solid tumor development. A phenotype representative of *in vivo* tumor progression was achieved in 3D *in vitro* bioengineered tumors by adjusting specific microenvironmental parameters, including limitingoxygen and nutrient diffusion and increasing competition for available nutrients. As the bioengineered tumors matured, *in*

vivo-characteristic regions of necrosis and hypoxia developed. The upregulation of VEGF-A gene expression in response to growing levels of intra-cellular hypoxia was a promising finding that may provide clinical relevance to this 3D *in vitro* bioengineered tumor model.

Acknowledgments

We would like to thank Andrea Martin for generously donating the Sprague Dawley rat tails. We also acknowledge our funding, which was provided by the NSF Early CAREER Award CBET 0955072 and the NIH/NHLBI R01HL098912.

References

1. Kim JB. Three-dimensional tissue culture models in cancer biology. Semin Cancer Biol. 2005; 15(5):365–77. [PubMed: 15975824]
2. Griffith LG, Swartz MA. Capturing complex 3D tissue physiology in vitro. Nat Rev Mol Cell Biol. 2006; 7(3):211–24. [PubMed: 16496023]
3. Yamada KM, Cukierman E. Modeling tissue morphogenesis and cancer in 3D. Cell. 2007; 130(4): 601–10. [PubMed: 17719539]
4. Horning JL, Sahoo SK, Vijayaraghavalu S, Dimitrijevic S, Vasir JK, Jain TK, et al. 3-D tumor model for in vitro evaluation of anticancer drugs. Mol Pharmacol. 2008; 5(5):849–62.
5. Hutmacher DW, Horch RE, Loessner D, Rizzi S, Sieh S, Reichert JC, et al. Translating tissue engineering technology platforms into cancer research. J Cell Mol Med. 2009; 13(8A):1417–27. [PubMed: 19627398]
6. Rangarajan A, Weinberg RA. Opinion: comparative biology of mouse versus human cells: modelling human cancer in mice. Nat Rev Cancer. 2003; 3(12):952–9. [PubMed: 14737125]
7. Kim JB, Stein R, O'Hare MJ. Three-dimensional in vitro tissue culture models of breast cancer– a review. Breast Cancer Res Treat. 2004; 85(3):281–91. [PubMed: 15111767]
8. Fischbach C, Chen R, Matsumoto T, Schmelzle T, Brugge JS, Polverini PJ, et al. Engineering tumors with 3D scaffolds. Nat Methods. 2007; 4(10):855–60. [PubMed: 17767164]
9. Cross VL, Zheng Y, Won Choi N, Verbridge SS, Sutermaster BA, Bonassar LJ, et al. Dense type I collagen matrices that support cellular remodeling and microfabrication for studies of tumor angiogenesis and vasculogenesis in vitro. Biomaterials. 2010; 31(33):8596–607. [PubMed: 20727585]
10. Nelson CM, Bissell MJ. Modeling dynamic reciprocity: engineering three-dimensional culture models of breast architecture, function, and neoplastic transformation. Semin Cancer Biol. 2005; 15(5):342–52. [PubMed: 15963732]
11. Nelson CM, Inman JL, Bissell MJ. Three-dimensional lithographically defined organotypic tissue arrays for quantitative analysis of morphogenesis and neoplastic progression. Nat Protoc. 2008; 3(4):674–8. [PubMed: 18388950]
12. Verbridge SS, Choi NW, Zheng Y, Brooks DJ, Stroock AD, Fischbach C. Oxygen-controlled three-dimensional cultures to analyze tumor angiogenesis. Tissue Eng Part A. 2010; 16(7):2133–41. [PubMed: 20214469]
13. Raof NA, Raja WK, Castracane J, Xie Y. Bioengineering embryonic stem cell microenvironments for exploring inhibitory effects on metastatic breast cancer cells. Biomaterials. 2011; 32(17):4130–9. [PubMed: 21411140]
14. Ghajar CM, Bissell MJ. Tumor engineering: the other face of tissue engineering. Tissue Eng Part A. 2010; 16(7):2153–6. [PubMed: 20214448]
15. Hutmacher DW, Loessner D, Rizzi S, Kaplan DL, Mooney DJ, Clements JA. Can tissue engineering concepts advance tumor biology research? Trends Biotechnol. 2010; 28(3):125–33. [PubMed: 20056286]
16. Szot CS, Buchanan CF, Gatenholm P, Rylander MN, Freeman JW. Investigation of cancer cell behaviour on nanofibrous scaffolds. Mater Sci Eng C. 2011; 31(1):6.
17. Hanahan D, Weinberg RA. The hallmarks of cancer. Cell. 2000; 100(1):57–70. [PubMed: 10647931]

18. Zhou J, Schmid T, Schnitzer S, Brune B. Tumor hypoxia and cancer progression. Cancer Lett. 2006; 237(1):10–21. [PubMed: 16002209]
19. Brahimi-Horn MC, Chiche J, Pouyssegur J. Hypoxia and cancer. J Mol Med. 2007; 85(12):1301–7. [PubMed: 18026916]
20. Kilarski WW, Bikfalvi A. Recent developments in tumor angiogenesis. Curr Pharm Biotechnol. 2007; 8(1):3–9. [PubMed: 17311548]
21. Hayes AJ, Huang WQ, Yu J, Maisonpierre PC, Liu A, Kern FG, et al. Expression and function of angiopoietin-1 in breast cancer. Br J Cancer. 2000; 83(9):1154–60. [PubMed: 11027428]
22. Bos R, van Diest PJ, de Jong JS, van der Groep P, van der Valk P, van der Wall E. Hypoxia-inducible factor-1alpha is associated with angiogenesis, and expression of bFGF, PDGF-BB, and EGFR in invasive breast cancer. Histopathology. 2005; 46(1):31–6. [PubMed: 15656883]
23. Bos R, Zhong H, Hanrahan CF, Mommers EC, Semenza GL, Pinedo HM, et al. Levels of hypoxia-inducible factor-1 alpha during breast carcinogenesis. J Natl Cancer Inst. 2001; 93(4):309–14. [PubMed: 11181778]
24. Saltzman, WM. Tissue engineering: principles for the design of replacement organs and tissues. New York: Oxford University Press; 2004.
25. Ala-aho R, Kahari VM. Collagenases in cancer. Biochim clin. 2005; 87(3–4):273–86.
26. Livak KJ, Schmittgen TD. Analysis of relative gene expression data using real-time quantitative PCR and the 2(−Delta Delta C(T)) Method. Methods. 2001; 25(4):402–8. [PubMed: 11846609]
27. Kenny PA, Lee GY, Myers CA, Neve RM, Semeiks JR, Spellman PT, et al. The morphologies of breast cancer cell lines in three-dimensional assays correlate with their profiles of gene expression. Mol Oncol. 2007; 1(1):84–96. [PubMed: 18516279]
28. Nagata S. Apoptotic DNA fragmentation. Exp Cell Res. 2000; 256(1):12–8. [PubMed: 10739646]
29. Whited BM, Whitney JR, Hofmann MC, Xu Y, Rylander MN. Pre-osteoblast infiltration and differentiation in highly porous apatite-coated PLLA electrospun scaffolds. Biomaterials. 2011; 32(9):2294–304. [PubMed: 21195474]
30. Paszek MJ, Zahir N, Johnson KR, Lakins JN, Rozenberg GI, Gefen A, et al. Tensional homeostasis and the malignant phenotype. Cancer Cell. 2005; 8(3):241–54. [PubMed: 16169468]
31. Levental KR, Yu H, Kass L, Lakins JN, Egeblad M, Erler JT, et al. Matrix cross-linking forces tumor progression by enhancing integrin signaling. Cell. 2009; 139(5):891–906. [PubMed: 19931152]
32. Provenzano PP, Inman DR, Eliceiri KW, Keely PJ. Matrix density-induced mechanoregulation of breast cell phenotype, signaling and gene expression through a FAK-ERK linkage. Oncogene. 2009; 28(49):4326–43. [PubMed: 19826415]
33. Ramanujan S, Pluen A, McKee TD, Brown EB, Boucher Y, Jain RK. Diffusion and convection in collagen gels: implications for transport in the tumor inter-stitium. Biophys J. 2002; 83(3):1650–60. [PubMed: 12202388]
34. Corstorphine L, Sefton MV. Effectiveness factor and diffusion limitations in collagen gel modules containing HepG2 cells. J Tissue Eng Regen Med. 2011; 5(2):119–29. [PubMed: 20653045]
35. Pampaloni F, Reynaud EG, Stelzer EH. The third dimension bridges the gap between cell culture and live tissue. Nat Rev Mol Cell Biol. 2007; 8(10):839–45. [PubMed: 17684528]
36. Sharpless NE, Depinho RA. The mighty mouse: genetically engineered mouse models in cancer drug development. Nat Rev Drug Discov. 2006; 5(9):741–54. [PubMed: 16915232]

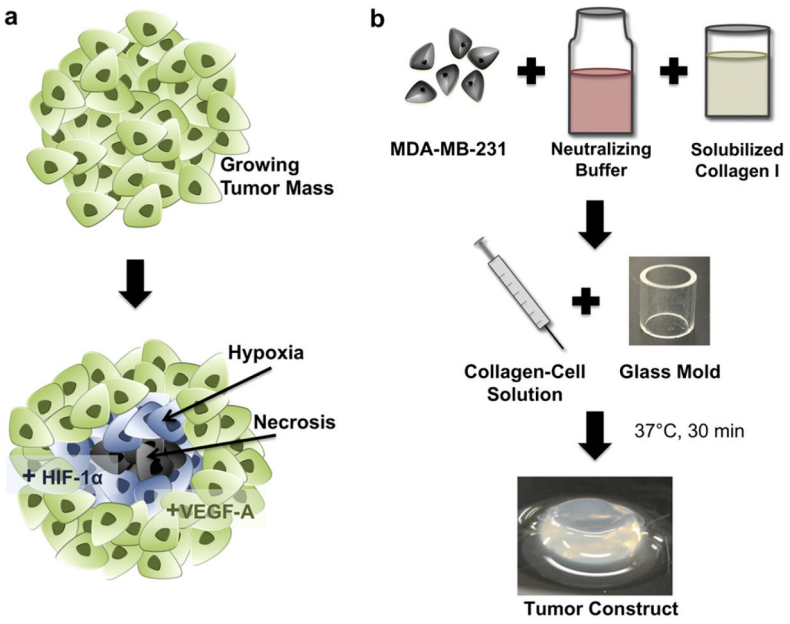

Fig. 1.

(a) The pre-vascularized stages of *in vivo* solid tumor development can be characterized by identifiable criteria within the tumor microenvironment, including an uninhibited 3D proliferative capacity, regions of hypoxia surrounding a necrotic core, and activation of angiogenic growth factors, including VEGF-A. (b) Collagen I hydrogels cultured with MDA-MB-231 human breast cancer cells were bioengineered as a platform for *in vitro* solid tumor development.

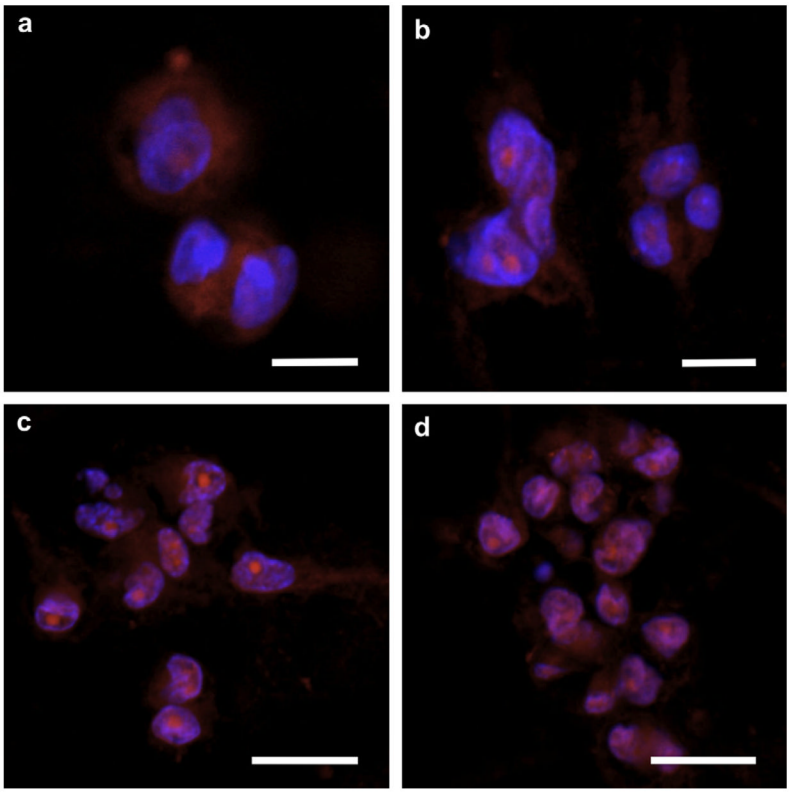

Fig. 2.

MDA-MB-231 cells were cultured in collagen I hydrogels for 1, 3, 5, and 7 days (a–d, respectively), exhibiting the typical cell-matrix and cell–cell interactions observed *in vivo*. Cells developed an elongated morphology over 7 days with visible processes, demonstrating cell-matrix interactions. As the cells began to proliferate, they aggregated into 3D clusters, demonstrating cell–cell interactions. Scale bars are (a, b) 10 μm and (c, d) 20 μm.

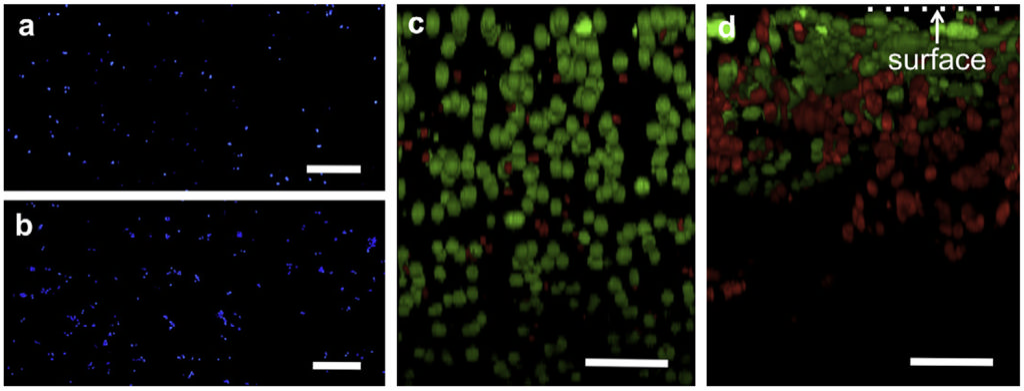

Fig. 3.

(a) MDA-MB-231 cells were seeded at a density of 1 million cells/ml, and on day 1, the cells were evenly distributed throughout the entire hydrogel. (b) Noticeable proliferation was observed on day 5, with cell proliferation leading to the formation of cell clusters. (c) The initial cell seeding density was increased to 4 million cells/ml, and on day 1, the viable cells (green) were evenly distributed with only a few dead cells (red) present at non-specific degrees of depth. (d) On day 5, cells were viable through ~150–200 μm of depth below the surface, with limitations in oxygen and nutrients leading to cell death towards the core of the bioengineered tumors. Scale bars are (a, b) 250 μm and (c, d) 100 μm. (For interpretation of the references to colour in this figure legend, the reader is referred to the web version of this article.)

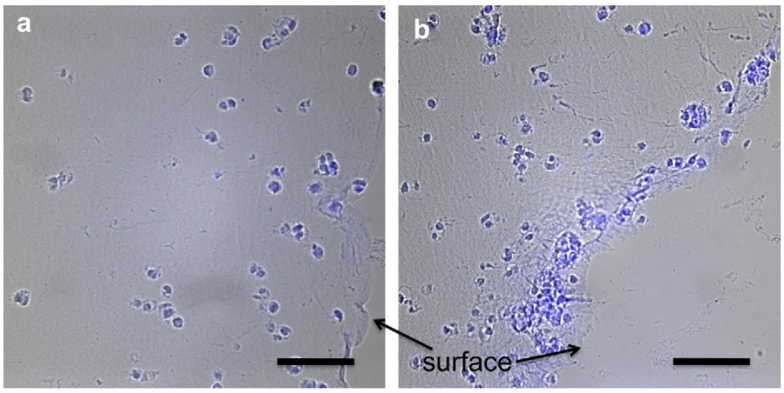

Fig. 4.

Hypoxia was detected using immunofluorescence for HIF-1α. (a) MDA-MB-231 cells were seeded at a density of 4 million cells/ml, and on day 1, the blue fluorescence indicated intra-cellular levels of hypoxia. (b) On day 5, the fluorescence intensity increased, in particular within the large cell clusters, signifying an increase in hypoxic oxygen levels. Scale bar is 100 μm.(For interpretation of the references to colour in this figure legend, the reader is referred to the web version of this article.)

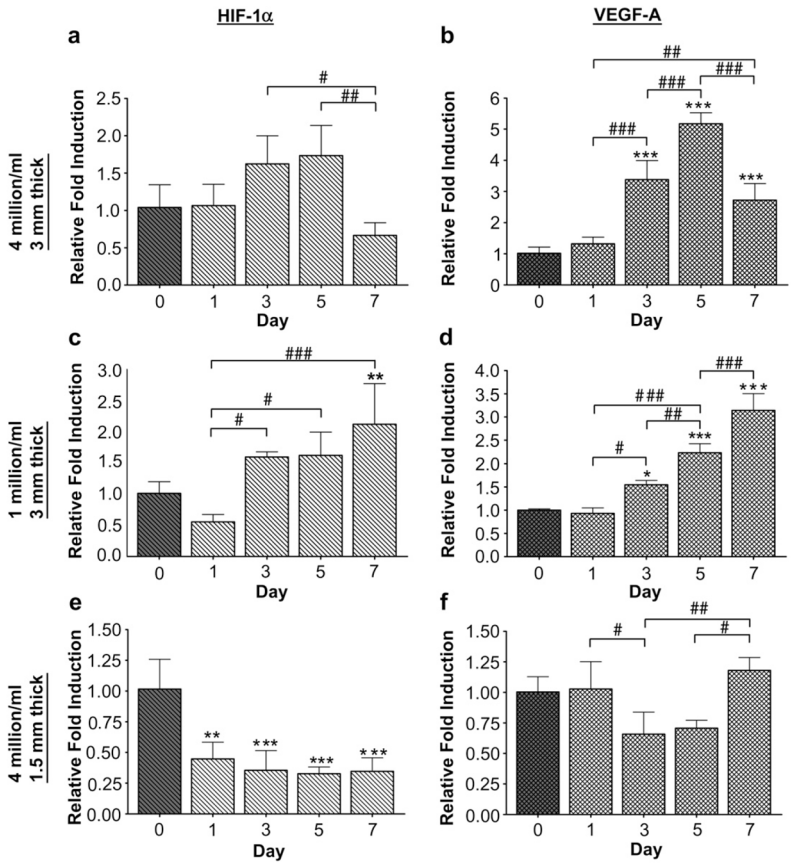

Fig. 5.

Quantitative RT-PCR was used to analyze the progression of HIF-1α and VEGF-A gene expression in the bioengineered tumors over a 7-day period, with expression on day 0 used as the control. (a, b) Similar to when both necrosis and hypoxia were observed, MDA-MB-231 cells were seeded at a density of 4 million cells/ml in 3 mm thick hydrogels. HIF-1α was upregulated on day 3 and day 5, and VEGF-A was significantly upregulated on days 3, 5, and 7. (c, d) When the initial cell seeding density was decreased to 1 million cells/ml, HIF-1α was significantly upregulated on day 7, and VEGF-A was significantly upregulated on days 3, 5, and 7. (e, f) When the cell seeding density was kept at 4 million cells/ml but a 1.5 mm thick hydrogel was used, neither HIF-1α nor VEGF-A were upregulated over the 7-day period. * was used to indicate significance compared to day 0. */#, **/##, and ***/### denote $p < 0.05$, 0.01, and 0.001, respectively.

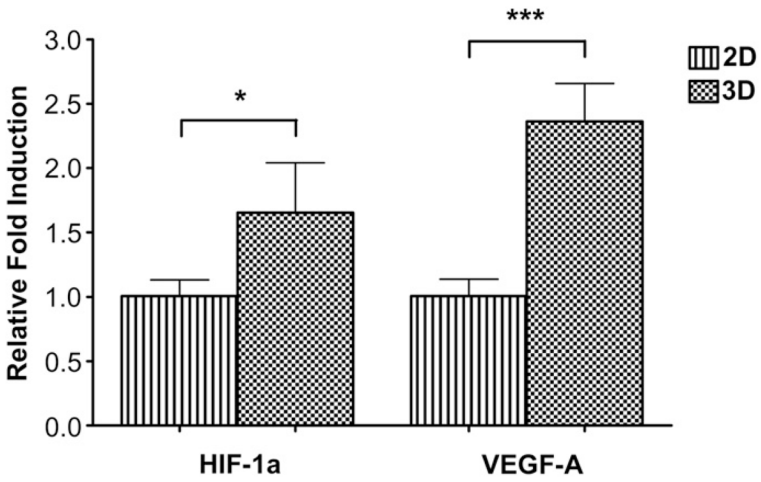

Fig. 6.

HIF-1α and VEGF-A gene expression were significantly upregulated when MDA-MB-231 cells were cultured in 3D collagen I hydrogels as compared to cells cultured in a monolayer on 2D tissue culture polystyrene. Gene expression was compared on day 0 to determine the specific effect of 3D culture without the contribution of cell proliferation or the development of hypoxia. * and *** denote $p < 0.05$ and 0.001, respectively.